Erschienen in: Physical Review Letters ; 120 (2018), 18. - 187401
https://dx.doi.org/10.1103/PhysRevLett.120.187401

Model Prediction of Self-Rotating Excitons in Two-Dimensional Transition-Metal Dichalcogenides

Maxim Trushin,[1,2] Mark Oliver Goerbig,[3] and Wolfgang Belzig[2]
[1]*Centre for Advanced 2D Materials, National University of Singapore, 6 Science Drive 2, 117546 Singapore*
[2]*Department of Physics, University of Konstanz, D-78457 Konstanz, Germany*
[3]*Laboratoire de Physique des Solides, Univ. Paris-Sud, Université Paris-Saclay, CNRS UMR 8502, F-91405 Orsay, France*

Using the quasiclassical concept of Berry curvature we demonstrate that a Dirac exciton—a pair of Dirac quasiparticles bound by Coulomb interactions—inevitably possesses an intrinsic angular momentum making the exciton effectively self-rotating. The model is applied to excitons in two-dimensional transition metal dichalcogenides, in which the charge carriers are known to be described by a Dirac-like Hamiltonian. We show that the topological self-rotation strongly modifies the exciton spectrum and, as a consequence, resolves the puzzle of the overestimated two-dimensional polarizability employed to fit earlier spectroscopic measurements.

Introduction.—An exciton is a bound electron-hole (e-h) pair optically excited in semiconductors. In most semiconductors, the electrons and holes behave like conventional Schrödinger quasiparticles and the corresponding exciton energy spectrum represents a hydrogenlike Rydberg series [1]. In contrast, the electrons and holes in two-dimensional (2D) transition-metal dichalcogenides (TMDs) mimic massive Dirac quasiparticles [2] resulting in an intrinsic quantum mechanical entanglement between conduction and valence band states as well as in a finite Berry curvature entering the quasiclassical equation of motion [3–6]. Moreover, the nonlocal screening of the Coulomb interactions in thin dielectric layers [7] suggests deviations from the conventional $1/r$ behavior at small e-h distances $r \sim r_0$, where $r_0 = 2\pi\chi$ is determined by the 2D polarizability χ [8]. Here, we show that both ingredients—the Berry curvature and the nonlocal screening—are crucial for a realistic exciton model aimed to describe the exciton energy spectrum in 2DTMDs. In what follows we employ a quasiclassical approach where the Berry curvature [3] and the 2D Keldysh potential [8] are taken into account on equal footing while quantizing the e-h relative motion. We utilize the model to fit the spectroscopic measurements for WS_2 [9] and WSe_2 [10], see Fig. 1, employing the only fitting parameter r_0. The resulting $r_0 \sim 4$ nm agrees with the *ab initio* prediction [11]. If the Berry curvature were neglected, r_0 has to be taken twice as large to fit the same spectra. This discrepancy has been pointed out by Chernikov *et al.* in Ref. [9], where $r_0 \sim 8$ nm has been employed. Our model is able to explain why the polarizability required to fit the measurements [9,10] is in fact twice smaller ($\chi \sim 0.7$ nm), in accordance with *ab initio* predictions [11]. The reason is that the Berry curvature results in a centrifugal-like term in the effective quasiclassical Hamiltonian, hence, reducing the quasiclassical phase space available for the relative e-h motion *as if* there were an additional angular momentum even for s states, see Fig. 2. In this sense, the excitons turn out to be self-rotating. The reduced phase space makes the energy level spacing smaller, similar to what the nonlocal screening (i.e., the Keldysh potential) does. In what follows we consider the model in detail.

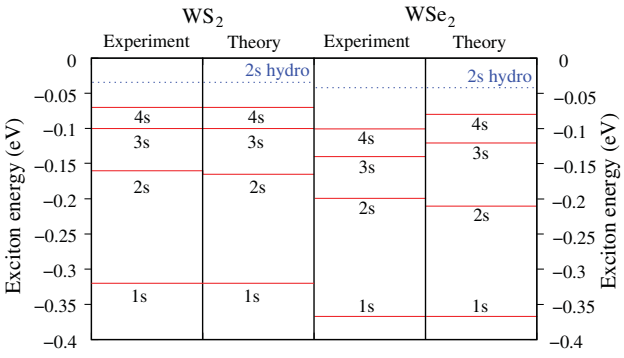

FIG. 1. Excitonic spectrum: measurements and theory. The experimental data have been taken from Refs. [9,10] for WS_2 and WSe_2, respectively. The theoretical spectra have been calculated quasiclassically from Eq. (15) taking into account nonlocal screening and self-rotation. Our theory employs reduced exciton masses $\mu = 0.16m_0$ for WS_2 and $\mu = 0.17m_0$ for WSe_2 (here, m_0 is the free electron mass) computed *ab initio* in Ref. [11]. We assume that the screening is due to the polarizability of the 2D layer $\chi = r_0/(2\pi)$ with r_0 being the only fitting parameter. In contrast to the conventional model [9] strongly overestimating r_0, we found that $r_0 = 4.65$ nm for WS_2 and $r_0 = 3.84$ nm for WSe_2, in agreement with the *ab initio* calculations [11] suggesting $r_0 \sim 4$ nm in such materials. Dotted lines show the first excited states ($2s$ states) within the standard hydrogenic model (6) to emphasize the qualitative difference with our findings.

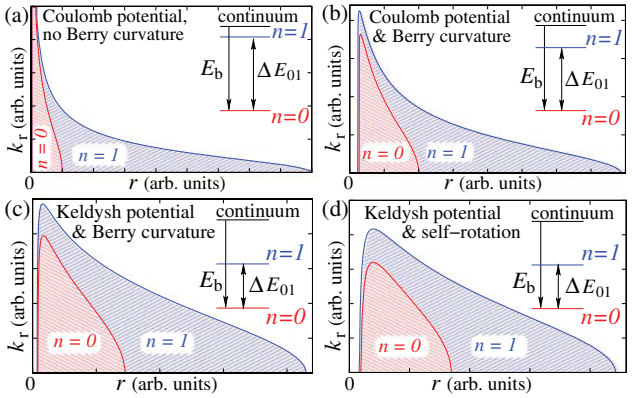

FIG. 2. The plots show the phase space available for relative quasiclassical motion of a massive Dirac e-h pair in the ground and first excited s states as well as the relative energy spacing between them. The relative spacing $\Delta E_{01}/E_b$ is proportional to the ratio between the two shaded areas. Parameters are taken to be relevant for WS_2. (a) Here, the Coulomb interaction with the effective dielectric constant $\epsilon = 5.2$ adjusted to fit the binding energy measured [9]. Neither the dielectric constant nor the level spacing turn out to be compatible with the values measured. (b) The Coulomb-Berry model results in a reduced phase space ratio and, as a consequence, reduced relative level spacing between the $n = 0$ and $n = 1$ states. The effective dielectric constant taken to fit the binding energy is twice smaller than in (a). (c) Both Berry curvature and Keldysh potential are taken into account on the same footing. The relative level spacing (and the phase space ratio) is reduced even stronger, matching the measured spectrum at the screening radius of a few nm. (d) An approximate model where the Berry curvature is emulated by an internal angular momentum $j = 1/2$ proving the concept of the self-rotating excitons in WS_2.

Approach.—The two-body problem for Dirac particles is not trivial [12–18] because of the intrinsic coupling between conduction and valence band states making the electron and hole states entangled even without Coulomb interactions. We employ an effective exciton Hamiltonian that accounts for this coupling and has several advantages over that proposed in Ref. [19]; see the Supplemental Material [20] for details. The Hamiltonian can be written as $H = H_0 + V(r)$, where $V(r)$ is the e-h interaction in relative coordinates, and H_0 is given by

$$H_0 = \begin{pmatrix} \frac{\hbar^2 k^2}{2\mu} & \hbar k\sqrt{\frac{\Delta}{2\mu}}e^{-i\theta} \\ \hbar k\sqrt{\frac{\Delta}{2\mu}}e^{i\theta} & \Delta \end{pmatrix}. \tag{1}$$

Here, Δ is the band gap, μ is the exciton reduced mass, and $\tan(\theta) = k_y/k_x$. The spectrum of H_0 has two branches: a single parabolic branch $E_k = \Delta + (\hbar^2 k^2/2\mu)$ describing excitonic states and, in contrast to Ref. [19], a dispersionless band $E_0 = 0$ being the vacuum state from which the excitons are initially excited. The corresponding eigenstates of H_0 can be written as $u_k = (\cos(\Phi/2), \sin(\Phi/2)e^{i\theta})^T$ and $u_0 = (\sin(\Phi/2), -\cos(\Phi/2)e^{i\theta})^T$, where $\tan(\Phi/2) = \sqrt{(2\mu\Delta/\hbar^2 k^2)}$. In order to make the model analytically tractable even for arbitrary $V(r)$ we rewrite H in the quasiclassical form [3]

$$H_{\rm exc} = \Delta + \frac{\hbar^2 k^2}{2\mu} + \frac{1}{2}\Omega\cdot(\nabla V \times k) + \frac{1}{4}\Omega\nabla^2 V + V(r), \tag{2}$$

where Ω is the exciton Berry curvature [21,22]. The latter can be computed as [23] $\Omega = \nabla_k \times \mathbf{A}$, with $\mathbf{A}$ being the Berry connection $\mathbf{A} = i\langle u_k|\nabla_k|u_k\rangle = -\sin^2(\Phi/2)\nabla_k\theta$. While the semiclassical expression (2) is general, the precise form of the quantum Hamiltonian (1) yields the particular Berry curvature $\Omega_z = \hbar^2\Delta/(\mu E_k^2) \simeq \hbar^2/(\mu\Delta)$ that is twice the one-particle Berry curvature [2,23,24], in agreement with Ref. [3]. The two-particle Berry curvature introduced here is a quantity describing the topology of an e-h pair, *not* of an electron and a hole separately. Since the potential $V(r)$ is circularly symmetric we employ cylindrical coordinates. To first order in $\partial_r V$, the total quasiclassical energy then reads

$$E_{\rm tot} = E_k + V(r) + \frac{\hbar^2\Delta}{2\mu r E_k^2}\frac{\partial V}{\partial r}\left(m + \frac{1}{2}\right), \tag{3}$$

where $m = 0, \pm 1, \pm 2, \ldots$ is the magnetic quantum number, and $E_k = \Delta + (\hbar^2/2\mu)[k_r^2 + (m^2/r^2)]$. One notices that the last term is due to the Berry curvature that couples the quantum number m and lifts the $m \leftrightarrow -m$ degeneracy as pointed out in Refs. [3,4]. The $1/2$ offset is furthermore due to the Darwin-like term $\Omega\nabla^2 V/4$ in Eq. (2), and one obtains the hydrogen model in the large-gap limit with $\Delta \to \infty$. Solving Eq. (3) with respect to the radial wave vector k_r, we then employ the Bohr-Sommerfeld quantization rule that in our case results in

$$\int_{r_1}^{r_2} k_r dr = \pi\left(n + \frac{1}{2}\right), \tag{4}$$

where $n = 0, 1, 2, \ldots$ is the radial quantum number and $r_{1,2}$ are the quasiclassical turning points. Note that there are in general six solutions for k_r but only one is real and positive. As we need only s states to compare with experiments, we set $m = 0$ everywhere from now on and consider a set of four models gradually approaching a simple but realistic one.

Coulomb model without Berry curvature.—This is the simplest exciton model possible, where the second term in Eq. (3) is neglected, and $V = -e^2/(\epsilon r)$. Equation (4) then explicitly reads

$$\int_{r_1}^{r_2} dr\sqrt{\frac{2\mu}{\hbar^2}\left(E_{\rm tot} - \Delta + \frac{e^2}{\epsilon r}\right)} = \pi\left(n + \frac{1}{2}\right), \tag{5}$$

where $r_1 = 0$, as there is no tangential momentum, see Fig. 2(a), and $r_2 = e^2/\epsilon(\Delta - E_{\rm tot})$. This results in the spectrum

$$E_n = \Delta - \frac{e^4\mu}{2\epsilon^2\hbar^2}\frac{1}{(n+1/2)^2}, \tag{6}$$

where $n = 0, 1, 2, \ldots$ is the radial quantum number. In order order to fit the binding energy for WS_2 (0.32 eV [9]) we have to take rather unrealistic effective dielectric constant $\epsilon = 5.2$. Moreover, the level spacing remains heavily overestimated, see Fig. 1 and Fig. 2(a). These observations all together indicate that the standard exciton model is not suitable for 2DTMDs.

Coulomb-Berry model.—Here, we retain the Berry curvature in Eq. (3), which for the Coulomb interaction reads

$$E_{\rm tot} = \Delta + \frac{\hbar^2 k_r^2}{2\mu} + \frac{e^2\hbar^2\Delta}{4\epsilon\mu r^3}\left(\Delta + \frac{\hbar^2 k_r^2}{2\mu}\right)^{-2} - \frac{e^2}{\epsilon r}. \tag{7}$$

$E_{\rm tot}$ contains now a centrifugal-like term that makes the phase space near $r = 0$ classically unavailable similar to what the conventional centrifugal term would do for $m \neq 0$. This is the most important intrinsic property of a self-rotating exciton that we believe to be crucial for a realistic model. Indeed, a real positive solution of Eq. (7) with respect to $\Delta + (\hbar^2 k_r^2/2\mu)$ (and, hence, with respect to k_r) is only possible when

$$E_{\rm tot} + \frac{e^2}{\epsilon r} \geq \frac{3}{2r}\sqrt[3]{\frac{\hbar^2 e^2 \Delta}{2\epsilon\mu}}. \tag{8}$$

As consequence, the e-h distance r cannot be smaller than r_1, where

$$r_1 = \frac{1}{E_{\rm tot}}\left(\frac{3}{2}\sqrt[3]{\frac{e^2\hbar^2\Delta}{2\epsilon\mu}} - \frac{e^2}{\epsilon}\right). \tag{9}$$

Since r_1 must be positive we find that the effective Bohr radius $r_B = \epsilon\hbar^2/(\mu e^2)$ must be larger than the effective Compton length $\lambda_C = \hbar/\sqrt{\mu\Delta}$. (The exact condition reads: $r_B > \lambda_C\sqrt{16/27}$.) The Compton length λ_C has a similar meaning here as in high-energy physics: It constitutes the cutoff below which spontaneous particle creation and annihilation processes become important and the concept of an exciton as a two-particle system is no longer valid. From the band theory point of view, this corresponds to the critical regime when the exciton binding energy approaches the size of the band gap. The realistic parameters we employ in Fig. 1 and Table I suggest that both λ_C and r_B are a few angstrom that makes our excitons strongly non-hydrogenic even if the interaction is Coulomb-like.

Note that the Berry curvature is hidden not only in the integrand of Eq. (4) but in its limits as well. On the one hand, this makes an explicit solution rather cumbersome but possible. Indeed, Eq. (7) can be solved explicitly with respect to k_r with the relevant branch given by

$$k_r = \sqrt{\frac{2\mu}{\hbar^2}\left(\frac{a}{3} + \frac{1+i\sqrt{3}}{6}c + \frac{2}{3}\frac{a^2}{(1+i\sqrt{3})c} - \Delta\right)},$$

where

$$c = \sqrt[3]{\frac{27b - 2a^3 - \sqrt{(27b-2a^3)^2 - 4a^6}}{2}},$$

and $a = E_{\rm tot} + e^2/(\epsilon r)$, $b = (e^2\hbar^2\Delta)/(4\epsilon\mu r^3)$. The lower limit is given by Eq. (9), whereas the upper limit can be *approximately* taken equal to r_2 given below Eq. (5). The latter is possible because the Berry term (being proportional to $1/r^3$) decreases much faster than the Coulomb potential at $r \to \infty$. On the other hand, the topological centrifugal effect occurs due to the *pseudospin*—the quantity associated with the 2×2 matrix structure of the effective Hamiltonian (1). Similar to the real spin the pseudospin can be seen as an internal angular momentum of our exciton. The explicit diagonalization of our initial Hamiltonian H has been performed in Ref. [25] within the shallow bound state approximation resulting in the s states spectrum given by

$$E_n = \Delta - \frac{e^4\mu}{2\epsilon^2\hbar^2}\frac{1}{(n+|j|+1/2)^2}, \tag{10}$$

where $j = 1/2$ is the pseudospin quantum number. In Table I we compare the exciton energy spectra calculated from Eqs. (10) and (4) and find very good agreement for all excited states. The models do not agree on the ground state energy because of at least two reasons: (i) The quasiclassical approximation is unreliable at low energies, (ii) the shallow bound state condition $(\Delta - E_n)/\Delta \ll 1$ may not be satisfied for $n = 0$. The latter may indeed take place for WSe_2 where the band gap $\Delta = 2.02$ eV [10] is somewhat smaller than in WS_2 ($\Delta = 2.41$ eV [9]) hence resulting in a

TABLE I. The $j = 1/2$ effective self-rotating exciton spectrum (10) is a good approximation for the quasiclassical Coulomb-Berry model introduced here. The dielectric constant is chosen to fit the binding energies E_b measured in Refs. [9,10]: $\epsilon = 2.6$ ($E_b = 0.32$ eV, $\Delta = 2.41$ eV) for WS_2, and $\epsilon = 2.5$ ($E_b = 0.37$ eV, $\Delta = 2.02$ eV) for WSe_2. The exciton reduced mass is the same as in Fig. 1.

$\lvert E_n - \Delta\rvert$, eV	$n=0$	$n=1$	$n=2$	$n=3$	$n=4$
WS_2 (self-rot.)	0.320	0.080	0.035(5)	0.020	0.0128
WS_2 (Berry)	0.315	0.081	0.036	0.020	0.013
WSe_2 (self-rot.)	0.370	0.0925	0.041(1)	0.023	0.014
WSe_2 (Berry)	0.344	0.0922	0.041	0.023	0.014

stronger discrepancy between the quasiclassical and quantum models.

Figure 2(b) shows how the Berry curvature reshapes the quasiclassically available phase space for the ground and lowest excited states. As compared to Fig. 2(a), the ratio between the two substantially decreases, hence, reducing the relative level spacing. If we again try to fit the binding energy for WS_2 by tuning the dielectric constant, we obtain the very reasonable number $\epsilon = 2.52$ close to what one expects for graphene on SiO_2 substrate ($\epsilon_{SiO_2} \sim 4$) with the upper surface exposed to air ($\epsilon_{Air} \sim 1$) resulting in $\epsilon \sim 2.5$. However, the level spacing is not reduced strong enough to describe the exciton spectra on a quantitative level. To improve the predictive power of our approach we change the screening model.

Keldysh-Berry model.—Until now we have assumed that the dielectric function is local in real space, i.e., q independent in reciprocal space. This is not true for 2D semiconducting systems, where the dielectric function is given by $\epsilon_q = 1 + 2\pi\chi q$ [8,26,27]. The real-space e-h interaction potential is known as the Keldysh potential [7] given by

$$V(r) = -\frac{\pi e^2}{2r_0}\left[H_0\left(\frac{r}{r_0}\right) - Y_0\left(\frac{r}{r_0}\right)\right], \tag{11}$$

where H_0 is the Struve function, Y_0 is the Bessel function of the 2nd kind, and r_0 is the screening radius being the only fitting parameter. The Berry term in Eq. (3) contains now $\partial_r V$ given by

$$\frac{\partial V}{\partial r} = -\frac{\pi e^2}{2r_0^2}\left[Y_1\left(\frac{r}{r_0}\right) + H_{-1}\left(\frac{r}{r_0}\right)\right]. \tag{12}$$

Because of the complexity of the r dependence in Eqs. (11), (12), it is no longer possible to obtain explicit expressions for $r_{1,2}$ in Eq. (4), but we can write the condition for the existence of real values of k_r:

$$E_{\text{tot}} - V(r) \geq \frac{3}{2}\sqrt[3]{\frac{\hbar^2\Delta}{2\mu r}\frac{\partial V}{\partial r}}. \tag{13}$$

One can see that this condition cannot be satisfied near $r = 0$, which again confirms the quasiclassical inaccessibility of this region as if there were a nonzero tangential momentum. The available phase space can be qualitatively evaluated from Fig. 2(c). The ratio between phase spaces available for the ground and 1st excited states is further reduced making the level spacing even smaller than in the Coulomb-Berry model. The absolute value of binding energy measured in Refs. [9,10] is matched at r_0 of a few nm compatible with *ab initio* calculations [11].

Self-rotating exciton model.—The Keldysh-Berry model while being realistic is too cumbersome for an express analysis of the experimental data. Aiming at a simplified model we employ the correspondence between the topological self-rotation and pseudospin angular momentum $j = 1/2$; see Table I. Generalizing this correspondence to any circularly symmetric potential, the quasiclassical energy for the excitonic s states can be written as

$$E_{\text{tot}} = \Delta + \frac{\hbar^2 k_r^2}{2\mu} + \frac{\hbar^2 j^2}{2\mu r^2} + V(r), \tag{14}$$

where $j = 1/2$ is the pseudospin angular momentum, and $V(r)$ is given by Eq. (11). The third term then mimics the Berry-curvature contribution and offers a good fit in the relevant intermediate-coupling regime, when $\alpha = e^2\sqrt{\mu/\Delta}/\hbar\epsilon \sim 1$ (or λ_C approaches r_B). However, it becomes less accurate when Δ is drastically increased ($\alpha \ll 1$) and the Berry curvature vanishes as $1/\Delta$. In the opposite limit of decreasing Δ the self-rotating model becomes again inapplicable as soon as Eq. (13) cannot be satisfied for a certain $r > 0$. This means that the system experiences an abrupt transition to a state that is no longer excitonic and that we do not aim to characterize here. The fitting model (14) does not describe this transition but matches the relevant physics once the system is *already* in a self-rotating regime, see the Supplemental Material [20] for details.

The quantization condition with the effective $j = 1/2$ self-rotation reads

$$\int_{r_1}^{r_2} dr\sqrt{\frac{2\mu}{\hbar^2}[E_{\text{tot}} - \Delta - V(r)] - \frac{j^2}{r^2}} = \pi\left(n + \frac{1}{2}\right), \tag{15}$$

where $r_{1,2}$ are determined by imposing the zero condition on the integrand. The qualitative justification of this model follows from Fig. 2(d): the quasiclassically available phase space appears to be very close to the one obtained within a somewhat more accurate approach depicted in Fig. 2(c). The major merit of the $j = 1/2$ effective model is its transparency in describing the self-rotation and non-Coulomb potential on the equal footing. It can easily be employed to fit the exciton spectra in Dirac materials [28] once they will be measured in future.

We use Eq. (15) to compute the energy for a given n; see Fig. 1. The model perfectly fits the exciton spectrum measured in WS_2 employing $r_0 \sim 4$ nm, as predicted *ab initio* in Ref. [11]. The agreement is less good in the case of WSe_2. This may be due to a certain incompatibility between the experimental data [9,10] and *ab initio* predictions [11]: The exciton binding energy measured in WSe_2 turns out to be higher than in WS_2, whereas the *ab initio* theory [11] predicts an opposite trend. Once the band gap $\Delta = 2.02$ eV (and, hence, the binding energy $E_b = 0.37$ eV) is reduced by a few tens of meV the exciton spectrum can be fitted for WSe_2 as good as for WS_2. However, we emphasize that our model fits

the data anyway much better than the conventional exciton model without Berry curvature.

Conclusion.—The very fact that the exciton spectrum in 2DTMDs [9,10,29] does not resemble the conventional Rydberg series has been discussed in multiple papers recently [3,4,14–17,27,30–38]. The commonly-accepted explanation [9] in terms of the nonlocal screening of the bare Coulomb potential [8] fits well the exciton spectrum measured [9] as long as an unrealistically high 2D polarizability is assumed. To cure this inconsistency, contributions from the Berry curvature need to be considered. The Berry curvature provides a strong repulsion when $r \to 0$ even for s states with no angular momentum. We have shown that this repulsion can be accounted for in a model where the excitons in 2DTMDs are *self-rotating* in a way similar to the quasiparticles on the surface of a strong topological insulator [22], thus opening further perspectives for excitonic engineering in van der Waals heterostructures [39].

We acknowledge financial support from the Center of Applied Photonics funded by the DFG-Excellence Initiative. M. T. was supported by the Director's Senior Research Fellowship from the Centre for Advanced 2D Materials at the National University of Singapore (NRF Medium Sized Centre Programme R-723-000-001-281). We thank Alexey Chernikov and Oleg Berman for discussions.

[1] R. J. Elliott, Phys. Rev. **108**, 1384 (1957).
[2] D. Xiao, G.-B. Liu, W. Feng, X. Xu, and W. Yao, Phys. Rev. Lett. **108**, 196802 (2012).
[3] J. Zhou, W.-Y. Shan, W. Yao, and D. Xiao, Phys. Rev. Lett. **115**, 166803 (2015).
[4] A. Srivastava and A. Imamoglu, Phys. Rev. Lett. **115**, 166802 (2015).
[5] P. Gong, H. Yu, Y. Wang, and W. Yao, Phys. Rev. B **95**, 125420 (2017).
[6] Z. R. Gong, W. Z. Luo, Z. F. Jiang, and H. C. Fu, Sci. Rep. **7**, 42390 (2017).
[7] L. V. Keldysh, Pis'ma Zh. Eksp. Teor. Fiz. **29**, 716 (1979).[JETP Lett. **29**, 658 (1979)].
[8] P. Cudazzo, I. V. Tokatly, and A. Rubio, Phys. Rev. B **84**, 085406 (2011).
[9] A. Chernikov, T. C. Berkelbach, H. M. Hill, A. Rigosi, Y. Li, O. B. Aslan, D. R. Reichman, M. S. Hybertsen, and T. F. Heinz, Phys. Rev. Lett. **113**, 076802 (2014).
[10] K. He, N. Kumar, L. Zhao, Z. Wang, K. F. Mak, H. Zhao, and J. Shan, Phys. Rev. Lett. **113**, 026803 (2014).
[11] T. C. Berkelbach, M. S. Hybertsen, and D. R. Reichman, Phys. Rev. B **88**, 045318 (2013).
[12] J. Sabio, F. Sols, and F. Guinea, Phys. Rev. B **81**, 045428 (2010).
[13] O. L. Berman, R. Ya. Kezerashvili, and K. Ziegler, Phys. Rev. A **87**, 042513 (2013).
[14] T. C. Berkelbach, M. S. Hybertsen, and D. R. Reichman, Phys. Rev. B **92**, 085413 (2015).
[15] F. Wu, F. Qu, and A. H. MacDonald, Phys. Rev. B **91**, 075310 (2015).
[16] G. Berghäuser and E. Malic, Phys. Rev. B **89**, 125309 (2014).
[17] T. Stroucken and S. W. Koch, J. Phys. Condens. Matter **27**, 345003 (2015).
[18] A. De Martino and R. Egger, Phys. Rev. B **95**, 085418 (2017).
[19] A. S. Rodin and A. H. Castro Neto, Phys. Rev. B **88**, 195437 (2013).
[20] See Supplemental Material at http://link.aps.org/supplemental/10.1103/PhysRevLett.120.187401 for justification of the effective Hamiltonian (1) and $j = 1/2$ self-rotating model.
[21] W. Yao and Q. Niu, Phys. Rev. Lett. **101**, 106401 (2008).
[22] I. Garate and M. Franz, Phys. Rev. B **84**, 045403 (2011).
[23] M. O. Goerbig, G. Montambaux, and F. Piéchon, Europhys. Lett. **105**, 57005 (2014).
[24] D. Xiao, W. Yao, and Q. Niu, Phys. Rev. Lett. **99**, 236809 (2007).
[25] M. Trushin, M. O. Goerbig, and W. Belzig, Phys. Rev. B **94**, 041301 (2016).
[26] S. Latini, T. Olsen, and K. S. Thygesen, Phys. Rev. B **92**, 245123 (2015).
[27] T. Olsen, S. Latini, F. Rasmussen, and K. S. Thygesen, Phys. Rev. Lett. **116**, 056401 (2016).
[28] T. Wehling, A. Black-Schaffer, and A. Balatsky, Adv. Phys. **63**, 1 (2014).
[29] H. M. Hill, A. F. Rigosi, C. Roquelet, A. Chernikov, T. C. Berkelbach, D. R. Reichman, M. S. Hybertsen, L. E. Brus, and T. F. Heinz, Nano Lett. **15**, 2992 (2015).
[30] M. Trushin, M. O. Goerbig, and W. Belzig, J. Phys. Conf. Ser. **864**, 012033 (2017).
[31] Z. Ye, T. Cao, K. O'Brien, H. Zhu, X. Yin, Y. Wang, S. G. Louie, and X. Zhang, Nature (London) **513**, 214 (2014).
[32] D. Y. Qiu, F. H. da Jornada, and S. G. Louie, Phys. Rev. Lett. **111**, 216805 (2013).
[33] A. Ramasubramaniam, Phys. Rev. B **86**, 115409 (2012).
[34] H.-P. Komsa and A. V. Krasheninnikov, Phys. Rev. B **86**, 241201 (2012).
[35] H. Shi, H. Pan, Y.-W. Zhang, and B. I. Yakobson, Phys. Rev. B **87**, 155304 (2013).
[36] T. Cheiwchanchamnangij and W. R. L. Lambrecht, Phys. Rev. B **85**, 205302 (2012).
[37] J. P. Echeverry, B. Urbaszek, T. Amand, X. Marie, and I. C. Gerber, Phys. Rev. B **93**, 121107 (2016).
[38] G. Wang, I. C. Gerber, L. Bouet, D. Lagarde, A. Balocchi, M. Vidal, T. Amand, X. Marie, and B. Urbaszek, 2D Mater. **2**, 045005 (2015).
[39] F. Wu, T. Lovorn, and A. H. MacDonald, Phys. Rev. Lett. **118**, 147401 (2017).